



Removal of ciprofloxacin antibiotic with nano graphene oxide magnetite composite: comparison of adsorption and photooxidation processes

Pelin Alicanoglu^a, Delia Teresa Sponza^{b,*}

^aPamukkale University, Engineering Faculty, Environmental Engineering Department, Kinikli-Denizli, Turkey, Tel. +90 258 296 30 42; Fax: +90 258 296 32 62; email: palicanoglu@pau.edu.tr

^bDokuz Eylul University, Engineering Faculty, Environmental Engineering Department, Buca-Izmir, Turkey, Tel. +90 232 301 71 19; Fax: +90 232 4531143; email: delya.sponza@deu.edu.tr

Received 13 April 2016; Accepted 18 August 2016

ABSTRACT

Ciprofloxacin (CIP) is a widely used fluoroquinolone antibiotic, both in aquatic life and agriculture. Graphene has been extensively utilized due to its favorable physical and chemical properties with a large surface area and high chemical and thermal stability. The aim of the study was to investigate the removal of CIP at increasing CIP and nano graphene oxide-magnetite (Nano-GO/M) composite concentrations, contact times and pH values by two different processes, namely adsorption and photooxidation. It was found that CIP removal by adsorption was low (maximum 15%–16.7%) at CIP concentrations between 1 and 1,000 mg/L, and the optimum operational conditions for these yields were 0.5–10 g/L Nano-GO/M composite, 30 min, and a pH of 6.5, respectively. The maximum adsorption capacities were between 2 and 2.2 mg_{CIP}/g_{Nano-GO/M} for 1 and 1,000 mg/L CIP concentrations, respectively. The CIP was mainly removed by the photodegradation process. For maximum removal of 1–3 mg/L CIP (93%–94%), the optimum Nano-GO/M composite concentration, contacting time and pH were found as 0.5 g/L, 30 min, and 6.5, respectively, by photooxidation at a power of 300 W. As the Nano-GO/M composite concentrations were increased from 0.5 g/L to 2 and 10 g/L, the CIP yields increased from 93%–94% to 95%–96% and 97%–98%, respectively, at an optimum pH of 6.5 after 30 min irradiation at 300 W. CIP was photodegraded according to the second-order reaction kinetic (0.088 min⁻¹). The calculated OH• radical concentrations were high at maximum CIP photodegradation yields. Under acidic and alkaline pH conditions, low CIP yields were obtained.

Keywords: Ciprofloxacin; Photooxidation; Adsorption; Retention time; Nano-composite

1. Introduction

Excessive use of pharmaceuticals has resulted in their detection in the effluents of wastewater treatment plants. Many of these pharmaceuticals have low biodegradability in the environment, and those absorbed by living creatures are disposed of from the living metabolism unchanged or little transformed. Among antibiotics in widespread use, fluoroquinolone antibiotics are an important type with undetectable biodegradability [1]. Ciprofloxacin (CIP) is a synthetic antibiotic used worldwide for the treatment of

several bacterial infections in both humans and animals. In receiving environments, low concentrations of antibiotic traces can cause resistance to microorganisms [2]. Concentrations of CIP in wastewaters have been obtained in the range from ng to mg/L (i.e., 50 mg/L near drug manufacturing plants) [3]; therefore, CIP removal from wastewater has become important. In the last literature surveys, a few studies have been reported for the removal of CIP from water, which include photooxidation [4], photo-Fenton oxidation [5], dissolved organic carbon [6], ozonation [7], montmorillonite [8], surface-modified carbon materials [9], adsorption onto biocomposite fibers of graphene oxide (GO)/calcium alginate [10] and adsorption on activated carbon [11].

* Corresponding author.

Graphene has the perfect sp^2 hybrid carbon nano-structure with a two-dimensional carbon structure. It also has excellent conductivity and a high specific surface area [12]. GO is a kind of novel two-dimensional graphene-based material, which was developed for the removal of pollutants in the aquatic environment which are dispersible and is beneficial for the removal of pollutants in wastewater because of different functional groups, such as hydroxyl, carboxyl and epoxy groups [13]. These functional groups make GO suitable for the removal of pharmaceuticals at a low cost. Chen et al. [14] studied the CIP removal with GO with initial 20 mg/L CIP concentration. 20 mg/L GO was used for sorption studies at $pH = 5$ after 1 h contact time. Removal of CIP was reported as 74%, and after 48 h sorption reached an equilibrium.

Magnetic Fe_3O_4 has an advantage for usage as a support material of composite adsorbents because it can be easily manipulated by an external magnetic field [15]. In recent literature surveys, there has been only one study about CIP removal by magnetite. Rakshit et al. [16] reported a study with nano-sized magnetite to remove CIP. They studied the effects of pH (in the range of 3.4–8.4) of ionic strengths (0.5, 0.1 and 0.01 M), and of initial CIP concentrations (in the range of 0.5–0.001 mM) on CIP adsorption using 10 g/L nano- $Fe_3O_4(s)$. The CIP was adsorbed via Freundlich isotherm with high R^2 values at 0.5, 0.1 and 0.01 M ionic strengths. They found that the sorption of CIP on nano- $Fe_3O_4(s)$ was strongly pH -dependent. In another study performed by Tang et al. [17], the maximum CIP adsorption capacity was recorded as 10.91 mg/g, which was investigated for 5 mg/L initial CIP concentration using 0.2 g/L reduced-GO/M concentration within 24 h retention time, at a pH of 6.2 and at a temperature of 25°C.

GO with large quantities of oxygen atoms on the surface is present in the forms of epoxy, hydroxyl and carboxyl groups. These functional groups make GO hydrophilic, and it is suitable to be an adsorbent [18]. Especially, some iron oxide nano-materials composited with GO as magnetic adsorbents are a better solution [18,19]. Thus, the combination of GO with magnetic nano-particles produces a magnetic graphene-based composite, which can be separated from the matrix rapidly and easily by an external magnetic field.

For the reason given above, in this study, the photocatalytic treatment and adsorption of CIP were studied with nano graphene oxide-magnetite (Nano-GO/M) composite. The effects of increasing Nano-GO/M composite concentrations developed under laboratory conditions, on increasing CIP concentrations, contacting times or irradiation times, acidic basic and neutral conditions on the yields of CIP adsorption capacity and on the photocatalytic removal efficiencies of CIP were studied and compared.

2. Materials and methods

2.1. Reagents and chemicals

CIP with a purity of >98% (Bayer AG, Germany), and graphene with a purity of 99% with a size of 1–3 μm and with a thickness, specific gravity and surface area of 0–9–1.2 nm, 1.4–2.0 g/cc and 40–300 m^2/g , respectively, were used (Aegean Nanotech Chemical Company, Izmir/Turkey). The purity, the size, the specific gravity, the surface area

and the density of magnetite used in this study were 99.9%, 20–30 nm, 1.9–2.2 g/cc, 80–100 m^2/g and 0.85 g/ cm^3 , respectively (Synergy Laboratory Products Ltd., Turkey). Demineralized water was used for the preparation of reagent solutions. 0.1 M HCl and 0.1 M NaOH were used to adjust the pH values of the CIP solutions.

2.2. Experimental procedures

2.2.1. Batch reactors for the adsorption process

The investigations were carried out in batch mode at increasing level pH , Nano-GO/M composite concentrations, contacting time and increasing CIP concentrations to obtain the maximum CIP yield for optimum adsorption conditions. The adsorption of CIP on the Nano-GO/M composite was studied using the batch adsorption technique. The adsorption experiments were conducted using 250 ml CIP solution of different initial CIP concentrations (1, 3, 5, 25, 100, 500 and 1,000 mg/L). The solutions were mixed with increasing Nano-GO/M composites (0.5, 2 and 10 g/L) in 1,000 mL Erlenmeyer glass flasks coated with Teflon placed on a rotating shaker at 150 rpm at a constant speed of 200 rpm and 22°C for 4 h to reach equilibrium (Fig. 1). Then, the wastewater samples

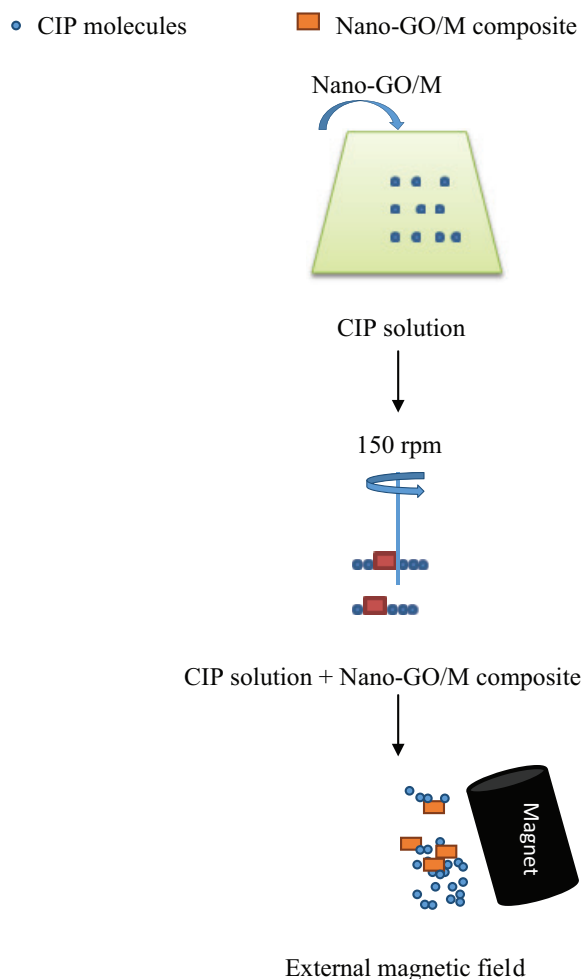


Fig. 1. Scheme of adsorption process.

were separated from the Nano-GO/M composite by an external magnetic field out of the glass Erlenmeyer flasks by using two magnets with dimensions of 10 cm × 6 cm. The pH of the CIP was adjusted between 4, 5, 6.5, 8 and 10 during the contact periods of 15, 30, 60 and 900 min. All experiments were done in duplicate.

The pH values, temperature and adsorbent dosage were identical for all of the equilibrium experiments in adsorption. During the adsorption process, samples were withdrawn from the reactors at certain time intervals. After magnetic separation, the amount of CIP adsorbed on the Nano-GO/M composite was calculated according to Eq. (1):

$$q_e = \frac{(C_0 - C_e) \cdot V}{W} \quad (1)$$

where C_0 and C_e (mg/L) are the initial and the equilibrium concentrations of CIP, respectively. V (L) is the volume of the solution, and W (g) is the mass of the adsorbent. The maximum CIP adsorption was investigated at increasing CIP concentrations (1–1,000 mg/L) using an optimum amount of Nano-GO/M composite and at optimum pH.

2.2.2. Quartz glass reactors for photocatalytic processes

Photocatalytic experiments were carried out in a closed and well-sealed system constructed from stainless steel material. Quartz glass reactors with dimensions of 38 cm × 3.5 cm and 10 UV lamps with a power of 30 W were placed into the closed stainless steel system for photocatalytic experiments (Fig. 2). The quartz glass reactors containing 50 mL of wastewater (approximately 0.50 cm of aqueous irradiated layer) were illuminated with a liquid surface of 80 mW cm⁻² within 315–400 nm at the mid-surface of the UV lamps, measured with a radiant power meter RM20 (Ettlingen, Germany). The experiments were carried out in triplicate. The solutions were mixed with increasing Nano-GO/M composites (0.5, 2 and 10 g/L).

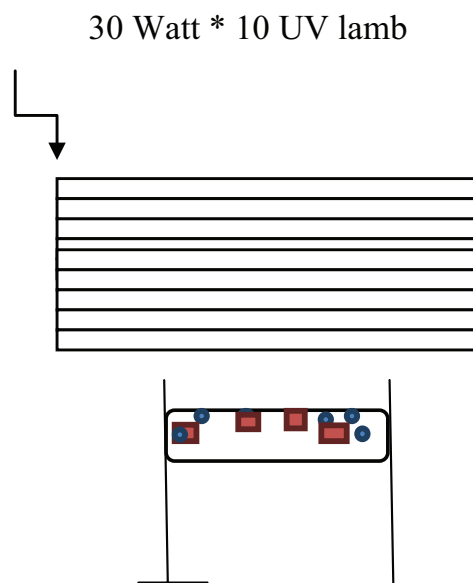


Fig. 2. Scheme of photocatalytic process.

The experiments were performed at increasing initial CIP concentrations (1, 3, 5, 25, 100, 500 and 1,000 mg/L), and the pH of the reaction mixture was adjusted from 4 to 10 using 1 M of H₂SO₄ and NaOH solution. Photocatalytic experiments were carried out with known quantities of Nano-GO/M composite varying between 0.5, 2 and 10 g/L at different irradiation times (15, 30, 60 and 900 min).

2.2.3. Synthesis of Nano-GO/M composite

In a typical synthesis, 5 g of purchased graphene was dispersed in 120 ml H₂SO₄ by adding 2.5 g of NaNO₃ to glass flasks coated with Teflon on a magnetic stirrer for 30 min placed in a water bath at a temperature of 18°C. After stirring the aforementioned mixture at a rpm of 500; 15 g of KMnO₄ was added gradually, and the last mixture continued to be stirred overnight, continuously, at 18°C. Then, 150 ml H₂O was slowly added and mixing continued for a day at 98°C. Finally, 50 mL of 30% H₂O₂ was added to the final mixture. The mixture was washed with 5% HCl and deionized water several times and, then, centrifuged and dried under vacuum for purification of the GO, which was obtained in a solid phase [20]. The Fe₃O₄ nano-particles were dispersed in 25 mL water and added to 50 mL GO aqueous solution. This mixture contained 1 mg Fe³⁺/1 mL GO, and it was stirred at 60°C through 1 h. The nano-composite was collected by using a magnet from the outside of the glass reactor, and it was washed with water three times [21].

2.3. Analytical procedures

CIP was measured using an high performance liquid chromatography (HPLC) (Agilent 1100). The HPLC consisting from a Pump, from an Auto-Sampler, from an HPLC Column from an oven and from an Diode-Array-Detector (DAD). The dimensions of C-18 thermo scientific column were 5 μm, 4.6 mm and 250 mm. The mobile phase consisted of KH₂PO₄ solution and acetonitrile (95:5, v/v). The flow rate was set at 1.5 mL/min, and the injection volume was 20 μL. The detection wavelengths of DAD were set at 210 nm. R² value of calibration graph of CIP was 0.999.

2.4. Calculation of [HO°]_{ss} concentrations

If we assume that HO° is the main species leading to photodegradation of CIP, the oxidation rate $V_{\text{CIP/HO}^\circ}$ (μg/mL/s) can be calculated using Eq. (2) [22]:

$$V_{\text{CIP/HO}^\circ} = -(\text{d}[\text{CIP}]/\text{d}t)_{\text{HO}^\circ} = k_{\text{CIP/HO}^\circ} [\text{CIP}] [\text{HO}^\circ]_{\text{ss}} \quad (2)$$

The degradation of CIP vs. photodegradation time was found to be pseudo-first-order with respect to CIP concentrations (Eq. (3)) [22]:

$$-(\text{d}[\text{CIP}]/\text{d}t) = k[\text{CIP}]_t \quad (3)$$

The degradation rates for all CIPs were deduced from the slopes of the curves derived from Eq. (4). In other words, the k values were calculated from the slope of the graphs plotted between $\ln([\text{CIP}]_t/[\text{CIP}]_0)$ and t .

$$\ln([CIP]_t/[CIP]_0) = k[CIP] \times t \quad (4)$$

The experimental rate of CIP photodegradation, $V_{CIP/US}$ ($\mu\text{g/ml/min}$), was calculated by using Eq. (5) [22]:

$$V_{CIP/US} = (d[CIP]/dt)_{US} = k[CIP] \quad (5)$$

The $[\text{HO}^\circ]$ concentration could be calculated by using Eq. (6):

$$[\text{HO}^\circ]_{ss} = k/k_{CIP/\text{HO}^\circ} \quad (6)$$

The second-order reaction kinetic rate constant for CIP ($k = 4.3 \times 10^{-9} \text{M}^{-1} \text{s}^{-1}$) was taken from the study performed by Yahya et al. [23].

2.5. Instrumental characterization

2.5.1. X-ray diffraction (XRD)

XRD analysis was carried out to investigate the phase and structure of Fe_3O_4 , GO and Nano-GO/M composite. XRD measurements were carried out with D/max-2200 PC (Rigaku, Japan), using $\text{Cu K}\alpha$ radiation.

2.5.2. Fourier transform infrared (FT-IR)

FT-IR spectra were carried out to recognize the functional groups in the synthesized composites and to confirm the chemical bonding between Fe_3O_4 and graphene. The FT-IR spectra of the Nano-GO/M before and after treatment conditions were measured with PerkinElmer FT-IR spectrum system using BX and KBr method.

2.5.3. SEM

The morphological and structural observation of raw and treated Nano-GO/M composite was made on a scanning electron microscope VegaII/LMU (Tescan, Czech Republic).

2.6. Photooxidation kinetic studies

2.6.1. First-order kinetics

A first-order reaction kinetic depends on the concentration of only one reactant (a unimolecular reaction). Other reactants can be present, but each will be zero order. The rate law for a reaction that is first order with respect to a reactant A is as follows:

$$\frac{-d[A]}{dt} \equiv r = k[A] \quad (7)$$

The integrated first-order rate law is as follows:

$$\ln[A] = -kt + \ln[A]_0 \quad (8)$$

A plot of $\ln[A]_0$ vs. time t gives a straight line with a slope of $-k$ [24].

2.6.2. Second-order kinetics

A second-order reaction kinetic depends on the concentrations of one second-order reactant, or two first-order reactants [24].

Its reaction rate is given as follows:

$$\frac{1}{[A]} = \frac{1}{[A]_0} + kt \quad (9)$$

3. Results and discussion

3.1. Psychochemical properties of Nano-GO/M composite

3.1.1. FT-IR analysis of Nano-GO/M composite

The raw Nano-GO/M composite produced and the Nano-GO/M composite that was used to photodegrade the 100 mg/L CIP after UV treatment were characterized using FT-IR. Fig. 3(a) shows the peaks of raw GO plotted between wave number (cm^{-1}) and percentage of transmittance (T-%). The peaks at 2,359 and 1,568 cm^{-1} show the characteristic spectrum of the benzene ring of the Nano-GO/M composite, while the peak at 1,073 cm^{-1} is the characteristic spectrum of the C–OH rings of the Nano-GO/M composite. The peak at 600 cm^{-1} is the characteristic of Fe_3O_4 , giving evidence of the successful preparation of the Nano-GO/M composite as reported by Huamin et al. [25]. Fig. 3(b) shows the FT-IR analysis of the Nano-GO/M composite after CIP treatment with UV. The maximum peaks obtained in this figure are similar to the nano-composite before UV treatment. Condensation of the Nano-GO/M composite remained almost the same after UV treatment. This shows that the Nano-GO/M composite can be recovered and can be used again for the treatment of CIP with UV.

3.1.2. XRD analysis of Nano-GO/M composite

XRD analysis was carried out to obtain the phase and structure of GO, Fe_3O_4 and Nano-GO/M composite before and after UV irradiation with 100 mg/L CIP concentration. As shown in Fig. 4, a series of characteristic peaks at the ranges at $2\theta = 30^\circ\text{--}32^\circ$, $35^\circ\text{--}37^\circ$, $43^\circ\text{--}45^\circ$, $53^\circ\text{--}55^\circ$, $57^\circ\text{--}59^\circ$ and $62^\circ\text{--}64^\circ$ vs. intensities (cps) were observed. These peaks were well matched to (220), (311), (400), (422), (511) and (440) of the crystal planes of Fe_3O_4 . Results showed that the Nano-GO/M composite was obtained successfully, and the crystalline structure of Fe_3O_4 did not change during the synthesis as reported by Nengsheng et al. [21].

3.1.3. SEM images of Nano-GO/M composite

The SEM images of synthesized GO, Fe_3O_4 nano-particles, raw and treated 0.5 g/L Nano-GO/M composites under UV for photodegradation of 100 mg/L CIP after 30 min irradiation under 300 W UV power at 21°C , are shown in Figs. 5(a)–(d), respectively. Fig. 5(a) shows the GO structure, which was in a sheet form. Fe_3O_4 nano-particles appear as small dots on the GO sheets (Fig. 5(a)). Many Fe_3O_4 microspheres were firmly anchored on both

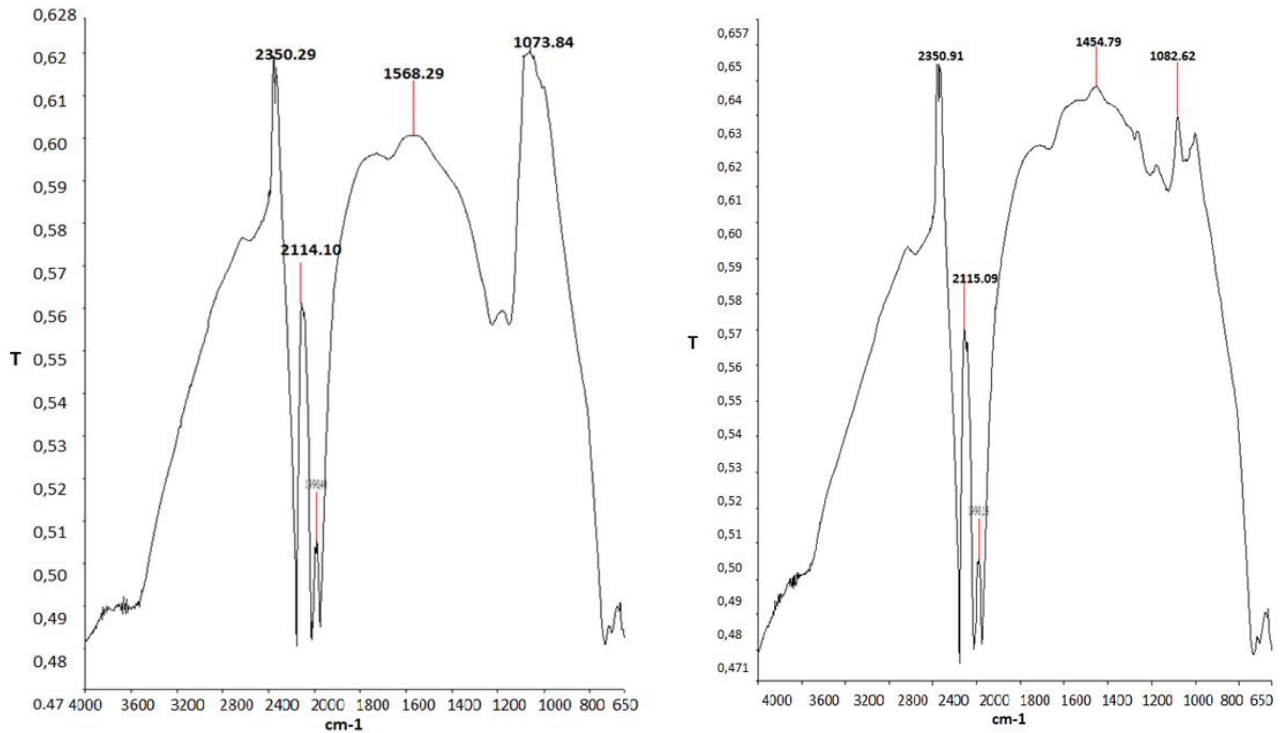


Fig. 3(a) FT-IR analysis of raw 0.5 g/L Nano-GO/M composite at 21°C and (b) FT-IR analysis of 0.5 g/L Nano-GO/M composite after photodegradation of 100 mg/L CIP at 30 min UV irradiation and at an UV power of 300 W.

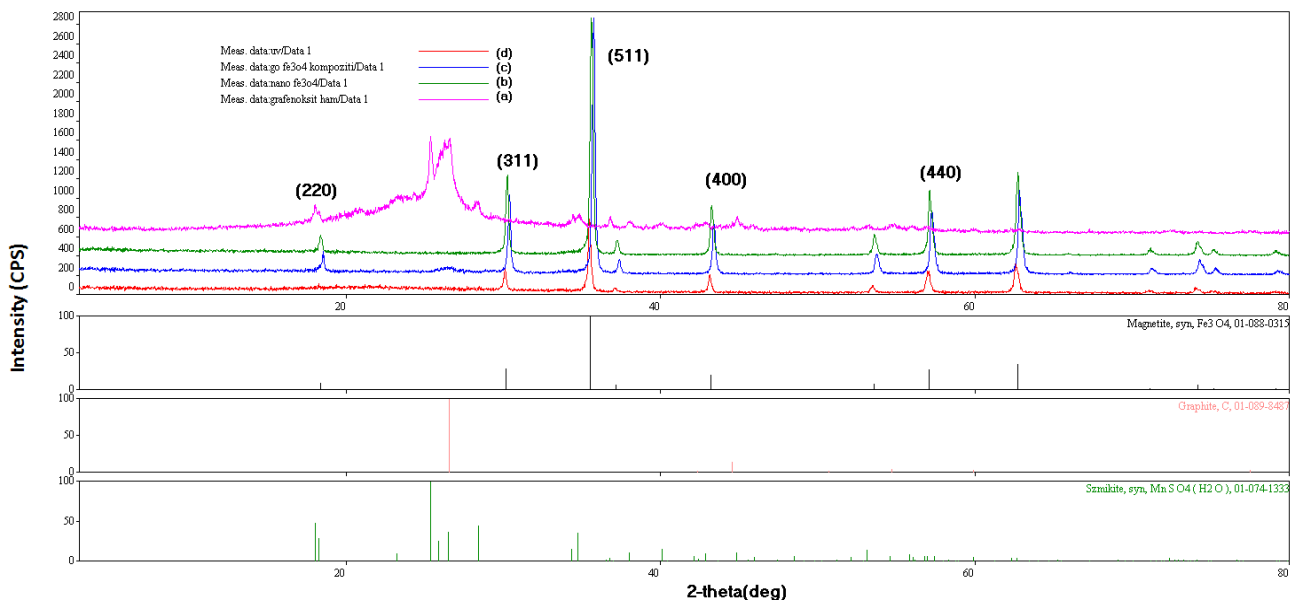


Fig. 4. XRD analysis of GO (a), Fe_3O_4 (b), raw 0.5 g/L Nano-GO/M composite (c), and 0.5 g/L Nano-GO/M composite after 30 min UV irradiation at 300 W, and 100 mg/L CIP concentration (d).

sides of the wrinkled graphene sheets (Fig. 5(c)). The graphene layers might contribute to preventing the Fe_3O_4 microspheres from forming aggregation, as reported by Tang et al. [17] (Fig. 5(c)). The Fe_3O_4 particles dispersed on GO, and there were some interspaces among them

[26] (Fig. 5(c)). After assembly, Nano-GO/M composites maintained their spherical morphology. Fe_3O_4 and GO were dispersed densely and evenly on the surface of the Nano-GO/M composites, and they had a core shell structure (Fig. 5(d)).

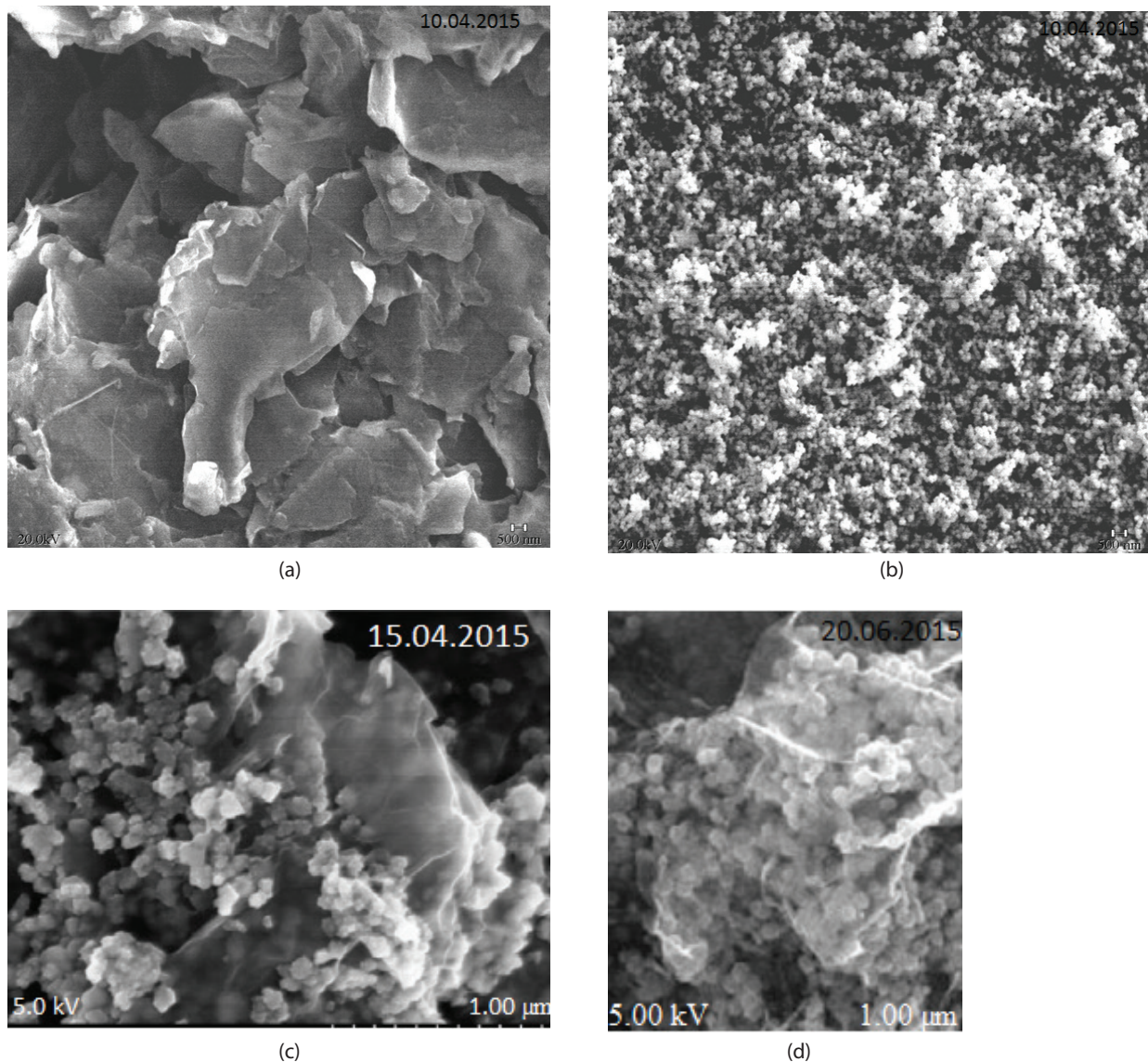


Fig. 5(a) SEM image of GO, (b) SEM image of nano-Fe₃O₄, (c) SEM image of raw Nano-GO/M before treatment, (d) SEM image of Nano-GO/M after UV irradiation.

3.2. Batch adsorption studies

3.2.1. Effects of Nano-GO/M composite concentrations on the treatment of CIP

In order to determine the maximum adsorption removal efficiencies of CIP (1, 3, 5, 25, 100, 500 and 1,000 mg/L), the effects of increasing Nano-GO/M composite concentrations (0.5, 2, and 10 g/L) were researched. The removal yields of 1 mg/L CIP via adsorption were found as 15%, 15.4% and 15.8% at 0.5, 2.0 and 10 g/L Nano-GO/M composite concentrations, respectively, after 30 min contact time at pH 6.5 and at a temperature of 21°C (Fig. 6). As the Nano-GO/M composite concentrations were increased from 0.5 g/L to 2.0 and 10 g/L, the CIP yields increased slightly. Since the cost of 2 and 10 g/L Nano-GO/M composite is higher than that of 1 g/L Nano-GO/M composite, and only slightly higher CIP yields were obtained, for maximum CIP adsorption yield

(15%), the optimum Nano-GO/M composite concentration was accepted as 0.5 g/L. As the CIP concentrations were increased from 1 mg/L to 3 and to 5 mg/L, the CIP adsorption yield increased slightly from 15% to 16.7% and 17% depending on increasing Nano-GO/M composite concentrations (from 0.5 g/L to 2.0 and 10 g/L), respectively. Further increases in CIP concentrations to 10, 25 and 1,000 mg/L did not increase the CIP yields in all Nano-GO/M composite concentrations. In this study, it is important to note that the adsorption yields of CIP on Nano-GO/M composite are very low both in low and high Nano-GO/M composite concentrations since the active sites on the surface of the Nano-GO/M are low and partially exposed to CIP. Therefore, low adsorption yields were obtained at all Nano-GO/M concentrations as reported by Li et al. [27]. The proposed mechanisms for the adsorption of organic substances on carbon materials mainly involve van der Waals forces (permanent

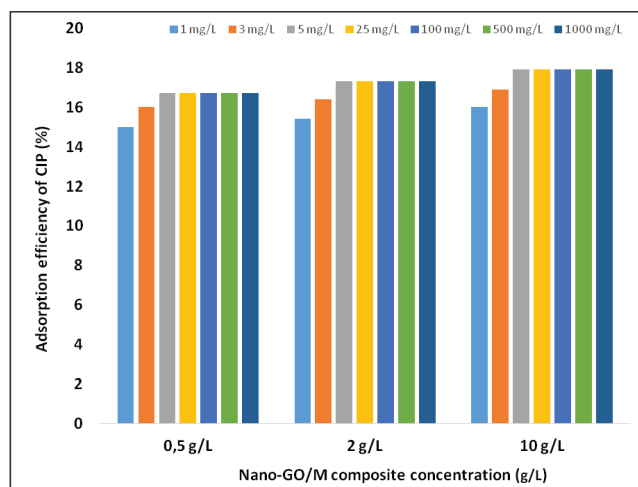


Fig. 6. Effect of increasing CIP concentration on the yields of CIP adsorption at Nano-GO/M composite concentration of 0.5, 2 and 10 g/L at pH = 6.5, at 21°C after 30 min contacting time.

dipole-induced dipole forces and London dispersion forces), hydrophobic interaction, π - π interaction (π was considered as one of the predominant driving forces due to the aromatic rings of CIP), electrostatic interaction and hydrogen bond [14].

The π - π interaction has always been applied to explain the binding mechanism of organic molecules such as CIP with C=C double bonds or benzene rings adsorbed on the surface of graphene. On the other hand, graphene also contains π electrons and may interact with the π electrons of benzene rings of CIP by means of π - π electron coupling [28]. Generally, the intensity of van der Waals forces between an adsorbed molecule (CIP) and adsorbent (Nano-GO/M composite) is related to the contacted surface area of them and to the van der Waals index, which is specific to the adsorbent surface [14]. The graphene surface of carbonaceous adsorbents has a very high van der Waals index, and the CIP molecule has a planar ring. However, no significant adsorption yields were obtained between the Nano-GO/M composite and CIP since no strong van der Waals forces occurred between CIP and the Nano-GO/M composite [14]. In the adsorption procedure, the π - π stacking interaction between the benzene rings of CIP molecule and the aromatic skeleton of the Nano-GO/M composite probably plays a key role in the adsorption of CIP to the Nano-GO/M composite [14].

There are few studies on the adsorption of CIP on GO in the literature, and the CIP adsorption yields were summarized as follows: the removal percentage of the 5 mg/L CIP reaches 68.9% at the adsorbent dose of 2 g/L and GO loading of 6%. The adsorption data fits well to the Freundlich model [29]. The adsorption capacity increased from 18.45 to 39.06 mg/g when the GO loading in the fibers was increased from 0% to 6% at the CIP equilibrium concentration of 60 mg/L [29]. Chen et al. [14] found that GO showed a strong adsorption to CIP (67%) with a maximum adsorption capacity of 320 mg/g. The interaction between GO and CIP can be controlled by different mechanisms, such as intraparticle diffusion due to charge screening effect, by electrostatic attacks and hydrogen bonding [14].

Carabineiro et al. [9] found maximum CIP adsorption capacities varying between 60 and 300 mg/g after 5 h adsorption time at 25°C, at a pH of 5 after 3 d equilibrium studies for oxidized carbon xerogel, and thermally treated activated carbon Norit ROX 8.0. Another study performed by Carabineiro et al. [30] showed that the adsorption capacities of CIP ranged from approximately 112 to 231 $\text{mg}_{\text{CIP}} \text{g}_{\text{C}}^{-1}$ for carbon xerogel and activated carbon, respectively. The CIP concentration decreased drastically in the first 5 h then a slow but gradual removal of CIP was observed until equilibrium was reached after 3 d. Usually, a longer period of time is needed for equilibrium, although small adsorbent particle sizes were used in the experiments to eliminate mass transfer limitations and accelerate the adsorption process, since the rate of adsorption is inversely proportional to the square of the adsorbent particle diameter. Although carbon sample also has micropores, a longer time is needed to reach adsorption equilibrium, due to the diffusion process that occurs in these kinds of pores. In our study, the adsorption capacities of Nano-GO/M composite varied between 2 and 2.2 $\text{mg}_{\text{CIP}}/\text{g}_{\text{Nano-GO/M}}$ as the CIP concentrations were increased from 1 to 1,000 mg/L CIP at a Nano-GO/M composite concentration of 0.5 g/L at pH = 6.5, at 21°C after 30 min contacting time. In other words, the maximum adsorption capacity of the Nano-GO/M composite was 2.2 $\text{mg}_{\text{CIP}}/\text{g}_{\text{Nano-GO/M}}$ after 30 min adsorption. The studies performed by Tang et al. [17] and Chen et al. [14] showed that the maximum adsorption capacities of CIP were 18.98 mg/l and 379–240 mg/g, respectively. These results showed that in our study the CIP adsorption capacity and the adsorption time required to reach steady-state conditions were comparatively lower with 0.5 g/L Nano-GO/M compared with the studies performed by Carabineiro et al. [9,30]. This may be attributed to a lower collision between CIP ions and active sites on the Nano-GO/M composite surface, to a lower driving force, which lowers the mass transfer and to some operational conditions such as pH, temperature and adsorbent production.

3.2.2. Effect of contacting time on the removal of CIP via adsorption

After determining the optimum Nano-GO/M composite concentration (0.5 g/L) for maximum CIP adsorption, it was decided to investigate the effects of contact time on the removal of 1 mg/L CIP at increasing retention times (15, 30, 60 and 90 min) with the original pH of the CIP solution (pH = 6.5) at a temperature of 21°C. The reaction time required to achieve adsorption equilibrium of CIP adsorption onto Nano-GO/M composite is important to evaluate the removal efficiency of the adsorbent materials. As the contacting time was increased from 15 to 30 min, the CIP removals by adsorption increased from 10% to 15% for an initial CIP concentration of 1 mg/L (Fig. 7). The adsorption process of CIP onto Nano-GO/M composite can be divided into two stages: (a) a rapid adsorption of CIP onto Nano-GO/M composite within 15 min of reaction time in which 10% CIP was removed with initial CIP concentration of 1 mg/L, and (b) a slow adsorption of CIP onto Nano-GO/M composite until an equilibrium was reached after 30 min with a maximum CIP yield of 15%. As the contacting time was increased from 30 min to 60 and 90 min, the CIP yields

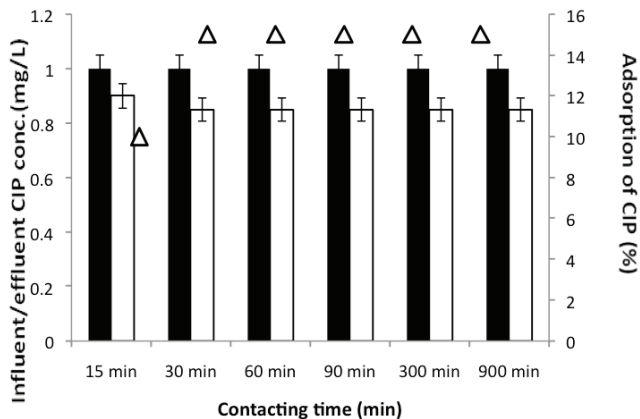


Fig. 7. Effect of contacting time on the yields of constant CIP concentration (1 mg/L), at a constant Nano-GO/M composite concentration (0.5 g/L), at a pH of 6.5 and at 21°C.

remained as in 30 min at all increasing CIP concentrations (1, 3, 5, 25, 100, 500 and 1,000 mg/L). The adsorption of CIP vs. contact time gives identical abrupt increases at low times before reaching the plateau. CIP adsorption equilibrium is achieved at 30 min. According to our literature survey, generally, adsorption of CIP onto Nano-GO/M is governed by three processes: (1) transport of CIP from solution to the surrounding of Nano-GO/M composite, (2) from the Nano-GO/M composite surface, and (3) from Nano-GO/M composite surface to the reactive sites [11].

3.2.3. Effect of increasing CIP concentrations on the CIP removal via adsorption

In this step of the study, the effects of increasing CIP concentrations (1, 3, 5, 25, 100, 500 and 1,000 mg/L) on the CIP removals via adsorption were studied at a Nano-GO/M composite concentration of 0.5 g/L, after 30 min contacting time, at pH = 6.5 and at a temperature of 21°C (Fig. 8). Results showed that increasing the CIP concentration slightly increased the removal efficiency of CIP at a Nano-GO/M composite concentration of 0.5 g/L. For 1 mg/L initial CIP concentration, the maximum CIP adsorption efficiency was found as 15% while the removal efficiency of 1,000 mg/L CIP was found 16.7%. As the CIP concentration was increased from 1 mg/L up to 3 and 5 mg/L, the CIP yields increased from 15% to 16% and 16.7%. Then the CIP yields remained stable as 16.7% for all CIP concentrations studied. For the maximum adsorption yield of CIP (16.7%), the maximum CIP concentration was found as 1,000 mg/L. As the CIP concentrations were increased, the adsorption efficiencies increased slightly. It is important to note that the CIP yield removed by adsorption was low both in low (1 mg/L) and high CIP (1,000 mg/L) concentrations. The reason for this can be explained as follows: at high CIP concentrations the surface of 0.5 g/L Nano-GO/M composite was not enough high to absorb all the CIP concentrations. Therefore, the adsorption efficiency was low at high CIP concentrations. In other words, Nano-GO/M composite adsorbs a small amount of CIP at high CIP (1,000 mg/L) concentrations, as reported by Hong et al. [31]. In this study, as opposed to the studies by Wang et al. [32], the CIP ions

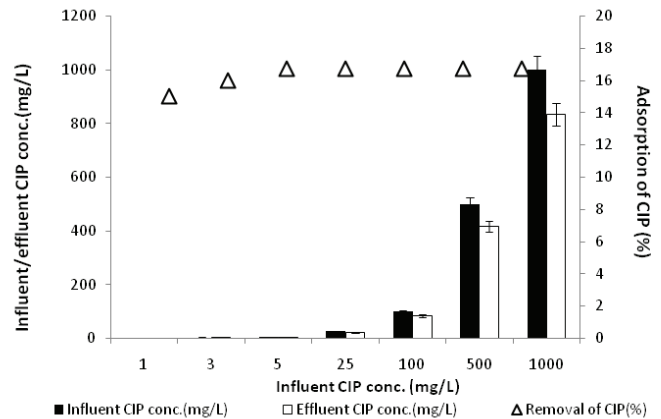


Fig. 8. Effect of increasing CIP concentration on the yields of CIP removal at a Nano-GO/M composite concentration of 0.5 g/L at pH = 6.5, at 21°C and 30 min contacting time.

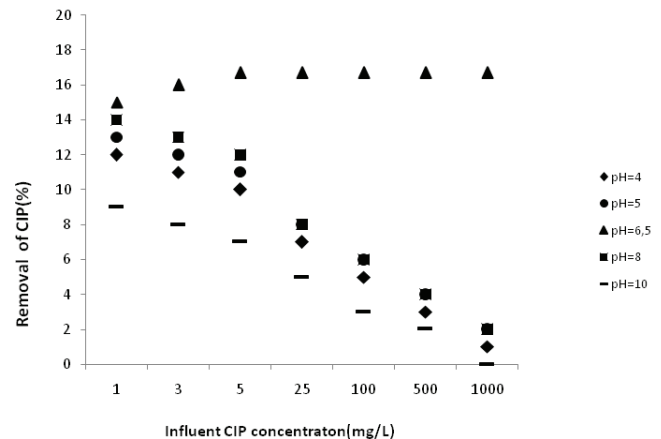


Fig. 9. Effect of different pH (4, 5, 6.5, 8 and 10) on the yield of CIP removal at a Nano-GO/M composite concentration of 0.5 g/L at pH = 6.5, at 21°C and 30 min contacting time.

around the absorbent sites of Nano-GO/M composite did not increase significantly with the increase of initial CIP concentration, indicating a low adsorption yield.

3.2.4. Effect of pH on the adsorption of CIP to Nano-GO/M composite

The effects of pH on the removals of CIP were studied under acidic, neutral and alkaline pH (4, 5, 6.5, 8 and 10) at an adsorption time of 30 min at a Nano-GO/M composite concentration of 0.5 g/L and at 21°C (Fig. 9). As the CIP concentration was increased from 1 mg/L to 3 and 5 mg/L, the adsorption yields increased from 5% to 16% and to 16.7% at pH = 6.5. Then as the CIP concentration was increased further up to 15, 100, 500 and 1,000 mg/L, the CIP yields remained the same. The maximum adsorption efficiency was found as 16.7% at pH = 6.5 at 1,000 mg/L CIP and 0.5 g/L Nano-GO/M composite concentration. As the pH values decreased from 6.5 to 5 and 4; the CIP adsorption yields decreased from 15% to 13% and 12% for 1 mg/L CIP concentration at

0.5 g/L Nano-GO/M composite concentration. Under alkaline conditions, also the adsorption yields decreased from 15% to 11% and 9% at pH 6.5, 8, and 10, respectively. CIP had positively charged (cationic; pH = 3), negatively charged (anionic; pH = 7.5), and/or zwitterionic (pH = 10) species due to different pKa of 6.1 and 8.7, respectively [33]. At pH < 6.1, CIP molecules mainly exist as cations (CIP⁺) because of the protonation of the amine group in the piperazine moiety of CIP [34]. At pH > 8.7, CIP molecules exist as anions (CIP⁻) due to the loss of a proton from the carboxylic group [35]. The zero charge point (pH_{pzc}) of the Nano-GO/M composite is at pH ≈ 5.5 [36,37]. Thus, the surface of Nano-GO/M composite was positively charged when pH < pH_{pzc} and negatively charged when pH > pH_{pzc}. As the pH increased from 4.0 to 5 and 6.5, the interaction between CIP and positively charged Nano-GO/M composite became more feasible. Above pH 6.5, both CIP and Nano-GO/M composite became increasingly negatively charged with increasing pH, resulting in decreased adsorption. As a result, maximum CIP adsorption was obtained at the original pH of CIP (pH = 6.5), as reported by Sponza and Oztekin [38].

3.3. Photocatalytic studies

The photocatalytic experiments were carried out at increasing Nano-GO/M composite concentrations (0.5, 2, and 10 g/L), at different pH values (4, 6.5 and 10) and at different irradiation times (15, 30, and 60 min) with a UV power of 300 W at CIP concentrations of 1, 3, 5, 25, 100, 500 and 1,000 mg/L.

3.3.1. Effects of increasing Nano-GO/M composite concentrations on the photoremoval of CIP by photooxidation

In this section, the effects of Nano-GO/M composite concentrations on the CIP photooxidation were investigated. The studies were performed at original pH of CIP = 6.5, at 21°C, at 30 min irradiation time, at 300 W UV light for an initial 1 mg/L CIP concentration. The removal efficiency was obtained as 93% at 1 mg/L CIP for 0.5 g/L Nano-GO/M composite (Fig. 10). 94% CIP photooxidation yield was obtained at 3 mg/L CIP for 0.5 g/L Nano-GO/M composite level (Fig. 10). As the CIP concentration was increased from 3 to 5 mg/L, the CIP yield remained the same (94%) for 0.5 g/L Nano-GO/M. Further increases in CIP concentration did not increase the CIP yields. The CIP yields at 25, 500 and 1,000 mg/L CIP concentrations remained as 94% at 0.5 g/L Nano-GO/M. With 2 g/L Nano-GO/M composite concentration, the CIP yields of 1, 3 and 5 mg/L CIP increased slightly to 95%, 96% and 97%, respectively, under the same operational conditions (Fig. 10). Then the CIP yields did not increase and remained as 97% for CIP concentration >5 mg/L. As the Nano-GO/M composite was increased to 10 g/L, the CIP yields of 1, 3 and 5 mg/L CIP concentrations were 97%, 98% and 98%, respectively. For maximum CIP yields (93%), the optimum Nano-GO/M composite concentration was accepted as 0.5 at 1 mg/L CIP concentration in order to decrease the cost of the nano-composite used. The photocatalytic treatment efficiency of 1 mg/L CIP increased with an increase in the Nano-GO/M composite dosage from 0.1 up to 0.5 g/L and increased slightly thereafter (data not shown). Increasing the amount of photocatalyst from 0.5 to 10 g/L resulted in a slight increase

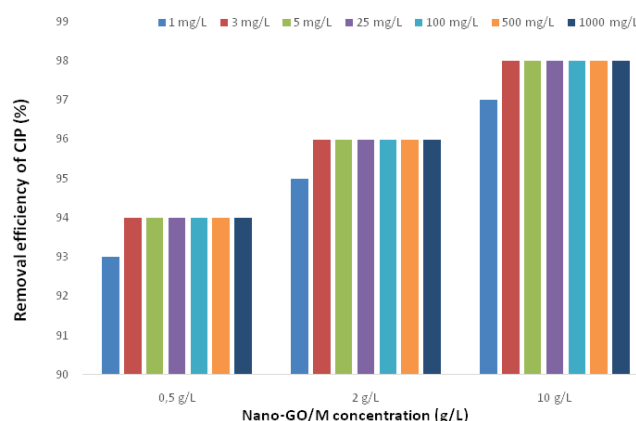


Fig. 10. Effect of increasing CIP concentration on the yields of CIP removal at a Nano-GO/M composite concentration of 0.5, 2 and 10 g/L at pH = 6.5, at 21°C and 30 min irradiation time by photooxidation under 300 W UV light.

in the photocatalytic treatment efficiency from 93% to 98% at an irradiation time of 30 min for 1 mg/L of CIP concentration, respectively. As the CIP concentrations were increased from 1 up to 3, 5, 25, 50 and 1,000 mg/L, the CIP photoremovals slightly increased from 93% to 94% up to 5 mg/L CIP concentration then the yields remained as 94% at 0.5 g/L Nano-GO/M composite concentration. At 2 g/L Nano-GO/M composite concentration, the CIP yields of 1, 3 and 5 mg/L CIP increased slightly to 95%, 96% and 97%, respectively. The CIP yields for >5 mg/L CIP concentrations remained as 97%. As the Nano-GO/M composite concentration was increased to 10 g/L, the CIP yields of 1, 3 and 5 mg/L CIP concentrations were 97%, 98% and 98%, respectively. Further increases in CIP concentration did not increase the CIP yields.

By increasing the catalyst concentration, the surface area was increased, leading to an increase in the production of reactive species [39]. As the Nano-GO/M concentration was increased from 1 g/L to 2 and 10 g/L, the CIP yields increased slightly. The reason for slightly higher CIP yields at a higher Nano-GO/M composite concentration (10 g/L) can be explained by the slight aggregation of the catalyst and partial increase in the total active surface area, thereby leading to a slightly increase in the photocatalytic treatment efficiency. Moreover, at a high nano-composite concentration, a reduction in the degree of light penetration can take place through the solution due to an increase in the turbidity of the solution [40]. Xinlin et al. [41] reported a maximum CIP (initial CIP concentration was 10 g/L) photocatalytic treatment efficiency of 70.90% for 0.1 g/L NaCl/GO-TiO₂ concentration within 60 min irradiation time, at a temperature of 30°C. In another study by Yan et al. [42], 68.2% photocatalytic CIP efficiency was obtained at 10 g/L initial CIP concentration using 2 g/L reduced-GO/BiVO₄ within 60 min irradiation time, at 30°C. Although the photocatalytic retention time is two times higher in the studies by Yan et al. [42] and Xinlin et al. [41], the CIP yields were higher in our study at 30 min. This could be attributed to the differences in adsorption kinetics, in driving force of the concentration gradients and to some operational conditions such as the UV light power and to the photoreactor configurations used in the studies.

3.3.2. Effect of irradiation time on the photooxidation of CIP

CIP treatment with Nano-GO/M composite was investigated at different irradiation times. Irradiation times were chosen as 15, 30, 60, 300 and 900 min. The concentration of Nano-GO/M composite was selected as 0.5 g/L to determine the optimum irradiation time since the maximum CIP removal was found in this nano-composite concentration as mentioned in section 3.3.1. The maximum removal efficiency of CIP was obtained at 60 min among the irradiation times used in the experiments. As the irradiation time was increased from 15 min to 30 and 60 min the CIP removals increased from 85% to 93% and 95% for initial CIP concentration of 1 mg/L (Fig. 11). Further increases in irradiation time from 60 min to 300 and 900 min did not increase the photodegradation efficiency of CIP and the saturation plateau was reached. CIP degradation initially underwent a fast increase and then the CIP removal efficiency remained as the same (95%) as the reaction continued for longer. A plausible explanation would be the generation of its oxidation products, which would compete with the parent compound for the oxidizing species and for the available radiation, and thus, the photodegradation yield after 300 and 900 min remained as it was at 60 min, as reported by Upadhyay et al. [43].

In the study performed by Lin and Wu [44], 10 mg/L CIP was photodegraded by the UV/S₂O₈²⁻ process with maximum removal yields of 50% and 69% after 5 and 30 min retention times, respectively. They also reported that after 30 min irradiation time the degradation efficiency did not show a significant increase, similar to our data. Yan et al. [42] reported that the CIP photodegradation efficiency was 68.2% after 60 min irradiation time with 20 mg reduced-GO-BiVO₄ composite for 1 mg/L CIP at 33°C in a photochemical reactor at an UV power of 300 W. In our study, at shorter irradiation times (30–60 min) than those in the study by Yan et al. [42], 93%–95% CIP removal yield was obtained for 1 mg/L CIP. According to the results obtained in this step of the study, it can be concluded that at very short (15–30 min) irradiation times lower CIP removal yields were obtained than at 60 min irradiation. This short retention time reduces the cost for photocatalytic removal of CIP to the Nano-GO/M composite. Thus, the optimum irradiation time for maximum CIP photooxidation was selected as 30 min.

3.3.3. Effect of pH on the UV treatment of CIP with Nano-GO/M composite

Due to the chemical nature of fluoroquinolones, pH is the parameter ruling the photodegradation of CIP onto the catalyst surface. The pH value is among the most important parameters that have an important impact on the photocatalytic capacity of the Nano-GO/M composite. The effects of pH on the increasing CIP concentrations (1, 3, 5, 25, 100, 500 and 1,000 mg/L) were studied under acidic, neutral and alkaline pH (4, 5, 6.5, 8 and 10) at an irradiation time of 30 min, at a Nano-GO/M composite concentration of 0.5 g/L and at 21°C. Photocatalytic removal efficiency of CIP on the Nano-GO/M composite was relatively high at pH 6.5. In this study, the maximum removal efficiency was found as 93% at pH = 6.5 at 1 mg/L CIP concentration and at 0.5 g/L Nano-GO/M composite concentration (Fig. 12). As the

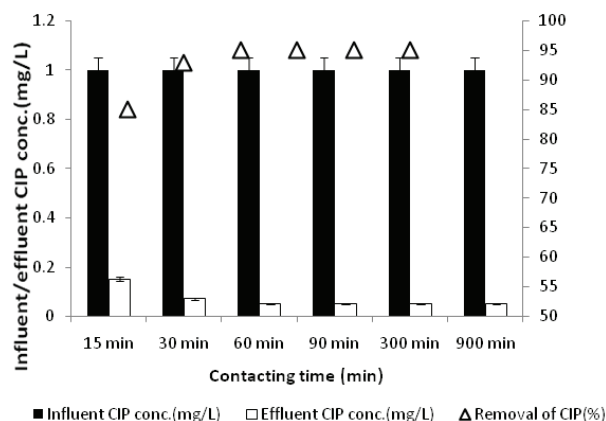


Fig. 11. Effect of irradiation time on the yields of constant CIP concentration (1 mg/L), at a constant Nano-GO/M composite concentration (0.5 g/L), at a pH of 6.5 and at 21°C.

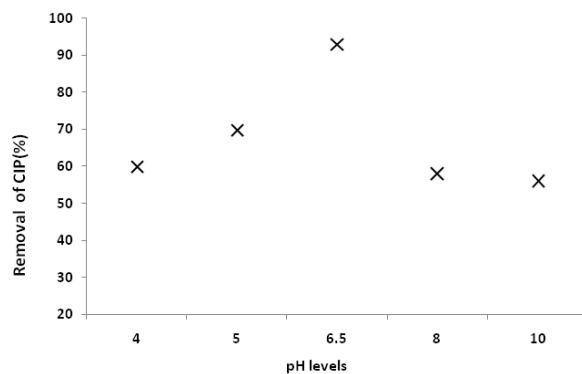


Fig. 12. Effect of different pH (4, 5, 6.5, 8 and 10) on the yield of CIP removal at a Nano-GO/M composite concentration of 0.5 g/L at pH = 6.5, at 21°C and 30 min irradiation time.

pH values decreased from 6.5 to 5 and 4 the CIP removal yields decreased from 93% to 70% and 60% at 1 mg/L CIP concentration at constant 0.5 g/L Nano-GO/M composite concentration. Under alkaline conditions, CIP photodegradation yields decreased from 93% to 58% and 56% for initial 1 mg/L CIP, at pH 6.5, 8 and 10, respectively, at an irradiation time of 30 min, at a Nano-GO/M composite concentration of 0.5 g/L and at 21°C and with 300 W UV light.

As the CIP concentrations were increased from 1 to 3 mg/L, the CIP removal yields increased from 93% to 94% at pH = 6.5 for 0.5 g/L Nano-GO/M. Further increases in CIP concentration did not increase the CIP yields at pH = 6.5 (Fig. 13). For CIP concentrations >3 mg/L, the CIP yields remained as 94% at pH = 6.5 for 0.5 g/L Nano-GO/M composite. Under acidic conditions (for pH = 5 and 4) as the CIP concentrations were increased from 1 to 3 mg/L, the CIP yield increased from 70% to 72%, respectively, at pH = 5.0. The CIP yields remained stable as 72% for CIP concentrations >3 mg/L (Fig. 13). The CIP yields decreased to 58%–59% at pH = 4.0. Under alkaline pH, the CIP yields still decreased. The CIP yields were 50%–52% and 46%–48% at pH = 8.0 and 10.0, respectively (Fig. 13). This can be a result of blocking of the photocatalytically active sites on the surface of Nano-GO/M composite by high CIP concentration under acidic and alkaline pH and reducing the

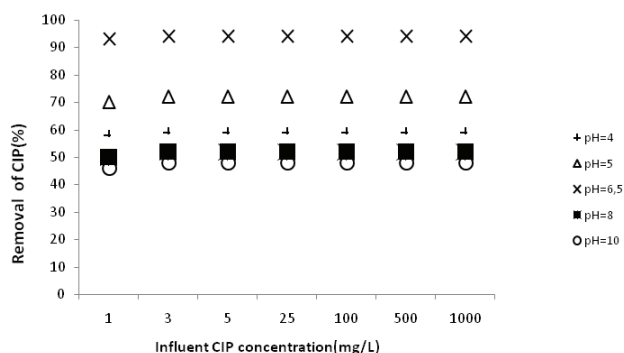


Fig. 13. Effect of increasing CIP concentrations on the yield of CIP removal at a Nano-GO/M concentration of 0.5 g/L at increasing pH (4–10), at 21°C and 30 min irradiation time with 300 W UV light.

interaction of photons with these sites as reported by Lin and Wu [44]. Hassani et al. [45] found that photodegradation efficiency increased at pH 5 under 200 W UV for the photocatalysis of 20 mg/L CIP with 0.1 g/L TiO_2 . These results are similar to our study. The low photodegradation efficiency at more acidic pH (e.g., at 4) may be related to the decomposition and corrosion of the catalyst in the acidic medium [46]. On the other hand, both Nano-GO/M composite and CIP were negatively charged in basic conditions, leading to electrostatic repulsion between them and the lower photodegradation efficiency of CIP. In the case of pH 6.5 (the natural pH of CIP), photocatalytic removal efficiency was the highest, and the surface of the Nano-GO/M was still in the positive form, and the CIP was in its neutral form [35].

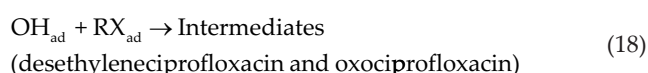
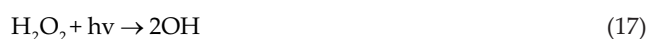
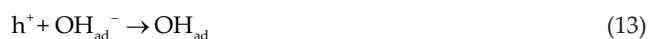
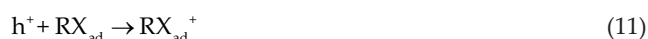
3.3.4. Effect of increasing CIP concentrations on the CIP removal by photooxidation

The effects of increasing CIP concentrations (1, 3, 5, 25, 100, 500 and 1,000 mg/L) on the CIP removals were studied at a Nano-GO/M composite concentration of 0.5 g/L, at 30 min irradiation time, under alkaline, neutral and acidic conditions at a temperature of 21°C under 300 W UV light (see Fig. 13). Results showed that increasing the CIP concentration yielded a slight increase in removal efficiency of CIP at a Nano-GO/M composite concentration of 0.5 g/L at pH = 6.5. For 1 mg/L initial CIP concentration, the maximum CIP removal efficiency was found as 93% while the removal efficiency of 1,000 mg/L CIP was found to be 94% at pH = 6.5 at 0.5 g/L Nano-GO/M composite concentration. The CIP yields remained stable as 94% after photocatalysis of 3 mg/L CIP (see Fig. 10). This can be a result of blocking of the photocatalytically active sites on the Nano-GO/M composite by increasing the CIP concentration and reducing the interaction of photons with these sites as reported by Lin and Wu [44]. Besides, the light absorbed by Nano-GO/M composite is low at a higher concentration of CIP, which can reduce the photocatalytic degradation efficiency to a certain extent [47]. Increased concentration of the CIP could occupy more active sites of the Nano-GO/M composite, which inhibits generation of the oxidants [48]. At a higher initial concentration, two factors could hinder the photodegradation of CIP: firstly, increased amount of CIP may occupy a greater number of active sites on the surface of the Nano-GO/M, which subsequently suppresses generation of the oxidants and results in lower degradation rates. Secondly, a higher

CIP concentration absorbs more photons, consequently decreasing available photons to activate the Nano-GO/M composite. Thus, a shortage of photons to activate the Nano-GO/M composite surface essentially retarded the degradation of CIP at high concentrations. Hence, the overall reaction rates remained similar with the higher initial CIP concentration compared with low CIP levels. This has been observed in many photochemical reactions where activation by photon absorption is typically the first step for a reaction [49].

3.3.5. CIP removal and produced OH^\bullet radical concentrations during photooxidation of CIP

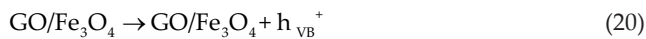
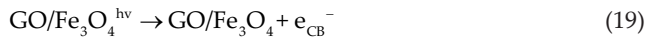
The photocatalytic oxidation of Nano-GO/M is presented in Eqs. (13)–(21). After receiving energy equal to or greater than the Nano-GO/M composite, an electron transfer to the conduction band leaving a hole in the valence band occurred. The electron and hole may recombine as one possibility. Another possibility is the reaction between photogenerated hole and water or hydroxide ion to form hydroxyl radicals.



High removal efficiency of CIP at pH = 6.5 with 0.5 mg/L Nano-GO/M concentration (93% for 1 mg/L CIP and 94% for CIP concentration of 3 mg/L and for CIP concentration >3 mg/L CIP, respectively), can be mainly attributed to the incorporation of GO into the magnetite composite catalyst. The GO can be accumulated on the active surface sites of magnetite and transfer the photogenerated electron (e_{CB}^-) into the conduction band of Fe_3O_4 efficiently. At the same time, a positively charged hole (h_{VB}^+) might be created by electrons migrating from the magnetite valence band to GO. This charge separation suppresses the recombination of h_{VB}^+ and e_{CB}^- , thus enhancing the photocatalytic activity of the composite catalyst. The h_{VB}^+ potential is positive enough to generate hydroxyl radicals by reacting with water, and e_{CB}^- potential is negative enough to produce superoxide radical anion by reducing absorbed molecular oxygen. The generated reactive hydroxyl radical and superoxide radical ions are responsible for the photocatalytic degradation of organic pollutants. Besides, the small amounts of Fe^{3+} ions dissolved from magnetite- Fe_3O_4 particles can come into not only

the electron capture position but also the hole capture position, which causes the electron-hole pair recombination of GO to decrease.

The role played by GO can be presented by Eqs. (19)–(22) as follows:



O_2 was dominantly produced in the water oxidation during photocatalysis with Nano-GO/M composite. The OH radical was produced as a by-product of the O_2 formation, where surface-adsorbed H_2O_2 in the form of Nano-GO/M composite was assigned as the reaction intermediate. The OH• radical concentrations during photocatalytic studies exhibited the degree of photocatalytic degradation. Table 1 shows the amount of OH• radical concentrations generated throughout photocatalytic degradation with and without the addition of the Nano-GO/M composite. The amount of OH• concentrations increased as the CIP and the Nano-GO/M composite concentrations were increased from 1 mg/L CIP to 3 mg/L. Further increases in CIP concentrations to 5, 25, 100, 500 and 1,000 mg/L did not affect the level of the OH• ion concentrations produced.

The OH• concentration increased from 1.9×10^{-3} $\mu\text{g/ml}$ to 2.0×10^{-3} and 2.2×10^{-3} $\mu\text{g/ml}$ at 1 mg/L initial CIP concentration as the Nano-GO/M composite concentrations were increased from 0.5 g/L to 2 and 10 g/L, respectively. The maximum OH• radical concentrations at 0.5 g/L

Nano-GO/M composite concentrations were observed at a CIP concentration of 3 mg/L and at CIP concentrations >3 mg/L for 5, 25, 500 and 1,000 mg/L CIP concentrations where the maximum CIP yields were obtained under 300 W and 30 min irradiation time (see Fig. 10 and Table 1). The OH• radical concentrations at 2 g/L Nano-GO/M composite concentration increased from 2.0×10^{-3} to 2.6×10^{-3} $\mu\text{g/ml}$. As the CIP concentrations were increased from 1 to 3 mg/L, the OH• radical concentrations remained stable as 2.6×10^{-3} $\mu\text{g/ml}$ after 3 mg/L CIP concentration. At 10 g/L Nano-GO/M composite, as the CIP concentrations were increased from 1 to 3 mg/L, the OH• radical concentrations increased from 2.2×10^{-3} to 2.9×10^{-3} $\mu\text{g/ml}$, respectively. At high CIP concentrations (>3 mg/L, up to 1,000 mg/L), the OH• radical concentrations remained stable as 2.9×10^{-3} $\mu\text{g/ml}$. The maximum OH• ion concentrations were obtained at a 10 g/L Nano-GO/M dose for 1 and 3 mg/L CIP concentrations. After 3 mg/L CIP concentration, the OH• ion levels remained stable at all Nano-GO/M concentrations.

The maximum OH• radical levels were obtained at pH = 6.5 and at a Nano-GO/M dose of 10 g/L at 1 and 3 mg/L CIP concentration (Table 1 and Fig. 13). Under 300 W UV without Nano-GO/M, the CIP removals were negligible. Without the nano-composite, the CIP degradation was not detected via UV illumination. In other words, no CIP photocatalysis was observed for CIP without the nano-composite.

Under UV irradiation, the generated electron transferred from the surface of Nano-GO/M composite to the CIP has always been considered as the first step of the photocatalytic action of nano-composites [47]. Photogenerated holes as well as hydroxyl radicals oxidize the CIP onto the surface of the Nano-GO/M composite. The high oxidative potential of holes can lead to direct and indirect oxidation of CIP. In the indirect oxidation process of CIP molecules, the hole at the valence band generates the hydroxide reactive radicals (OH•) via reaction with water and/or hydroxide anions (OH•).

Table 1

Produced OH• radical concentrations ($\mu\text{g/ml}$) vs. used Nano-GO/M composite concentrations under different operational conditions during photocatalysis

CIP Concentration (mg/L)	Nano-GO/M concentration (0 g/L), 300 W UV, pH = 6.5 after 30 min irradiation time					
	OH• radical concentrations ($\mu\text{g/ml}$) produced during photocatalysis			CIP removal efficiency (%)		
1	0			0.9		
10	0			0.6		
Influent CIP Concentration (mg/L)	Nano-GO/M composite concentrations used (g/L), 300 W UV at pH = 6.5 after 30 min irradiation time			Nano-GO/M composite concentrations used (g/L)		
	0.5	2	10	0.5	2	10
	OH• radical concentrations ($\mu\text{g/ml}$) produced during photocatalysis			CIP removal efficiency (%)		
1	1.9×10^{-3}	2.0×10^{-3}	2.2×10^{-3}	93	95	97
3	2.4×10^{-3}	2.6×10^{-3}	2.9×10^{-3}	94	96	98
5	2.4×10^{-3}	2.6×10^{-3}	2.9×10^{-3}	94	96	98
25	2.4×10^{-3}	2.6×10^{-3}	2.9×10^{-3}	94	96	98
100	2.4×10^{-3}	2.6×10^{-3}	2.9×10^{-3}	94	96	98
500	2.4×10^{-3}	2.6×10^{-3}	2.9×10^{-3}	94	96	98
1,000	2.4×10^{-3}	2.6×10^{-3}	2.9×10^{-3}	94	96	98

Under UV irradiation, the generated electron transferred from the surface of Nano-GO/M composite surface to the adsorbed CIP has always been considered as the first step of the photocatalytic action of nano-composites [49]. Photogenerated holes as well as hydroxyl radicals oxidize the CIP adsorbed at the Nano-GO/M composite surface. The high oxidative potential of holes can lead to direct and indirect oxidation of CIP. In the indirect oxidation process of CIP molecules, the hole at the valence band generates hydroxide reactive radicals (OH•) via a reaction with water and/or hydroxide anions (OH•). The species photon-generated holes, and electrons and hydroxyl radicals (OH•) can thus degrade CIP to intermediates, namely M1 (desethyleneciprofloxacin) and M3 (oxociprofloxacin). From 1 mg/L CIP, 0.2022 mg/L M1 and 0.034 mg/L M3 were produced as metabolites of photodegraded CIP (data not shown).

3.3.6. Recovery of Nano-GO/M

To investigate the repeatability of Nano-GO/M composite activity, recycling experiments were carried out (Fig. 14). After the completion of the degradation, the catalyst was collected, washed, dried at 200°C for 2 h and utilized for the next cycle by keeping other reaction conditions constant. After five cycles, the composite photocatalyst showed a slight drop in catalysis efficiency from 93% to 88%. This indicated that the photocatalytic activity of the Nano-GO/M composite catalyst had good repeatability. The reduction in the photocatalytic degradation efficiency among the cycles may be due to the fouling of the catalyst by the generated by-products during the photocatalysis reaction. By using a magnet (2 cm × 2 cm), the Fe₃O₄ nano-particles were separated from Nano-GO/M composite because Fe₃O₄ nano-particles involved in our system show a super-paramagnetic property, which can favor the composites re-dispersing in the water after magnetic separation.

3.3.7. Investigation of photodegradation kinetics of CIP using Nano-GO/M composite

In this step of the study, first-order and second-order kinetic models were discussed to indicate the removal kinetics of CIP on the surface of Nano-GO/M composite

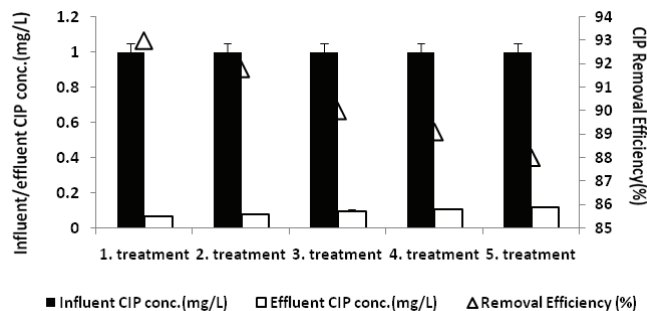


Fig. 14. Recovery of Nano-GO/M for 1 mg/L CIP concentration, at a Nano-GO/M composite concentration of 0.5 g/L at pH = 6.5, at 21°C and 30 min irradiation time with 300 W UV light.

throughout photodegradation under UV. In the first-order kinetic, the R^2 value of the linear line was 0.933. The reaction of the first order in the first-order rate kinetic constant is k_1 . The k_1 value was evaluated from the first-order reaction plots, and it was calculated as 0.074 min⁻¹ for CIP (Fig. 15(a)). The R^2 value for the second-order reaction was found as 0.969 for CIP in the photocatalytic studies performed with the Nano-GO/M composite (Fig. 15(b)). The reaction of the second order in the second-order rate kinetic constant is k_2 . The k_2 value was evaluated from second-order reaction plots, and it was found as 0.088 min⁻¹ for CIP. It was found that the second-order photocatalytic reaction kinetic with high R^2 values is meaningful and adequate to define the photocatalytic degradation of CIP. This high rate constant suggests that CIP can be degraded fast via a photocatalytic process [49]. Based on the high second-order kinetic constant (k_2 : 0.088 min⁻¹), it can be said that Nano-GO/M composite exhibits good photocatalytic activity to degrade the CIP under UV light irradiation. Tang et al. [17] observed that the photodegradation of CIP antibiotic on Nano-GO/M obeyed the pseudo-second-order kinetics (k_2 : 0.013 min⁻¹). The pseudo-second-order model assumed that the adsorption capacity was proportional to the number of active sites on the nano-composite during photocatalysis [17]. Furthermore, Chen et al. [14] found that the CIP photodegradation on Nano-GO/M exhibited a second-order reaction kinetic (k_2 : 0.004 h⁻¹). The differences in the second-order reaction kinetics can be attributed to the CIP concentrations used, to the Nano-GO/M preparation and to the environmental and operational conditions such as temperature, UV light power and pH.

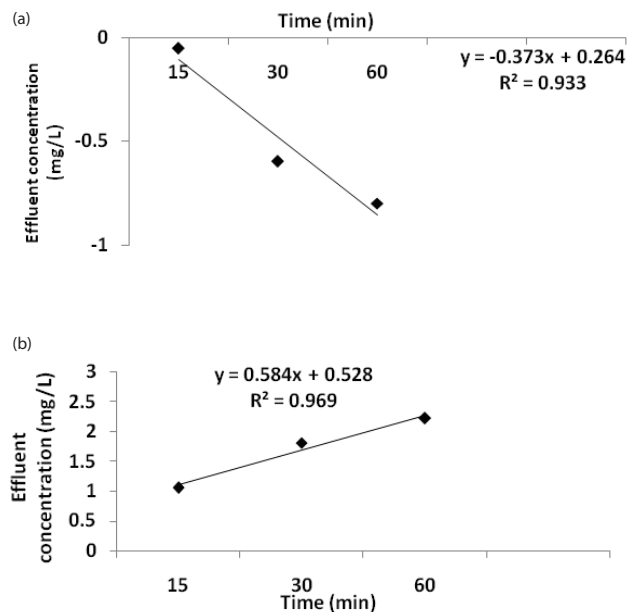


Fig. 15. (a) First-order reaction of CIP (CIP concentration: 5 mg/L, at room temperature, irradiation time: 30 min, concentration of Nano-GO/M composite: 0.5 g/L, 300 W UV light) and (b) second-order reaction of CIP (CIP concentration: 5 mg/L, T: room temperature, irradiation time: 30 min, concentration of Nano-GO/M composite: 0.5 g/L, 300 W UV light).

4. Conclusion

Adsorption and the photocatalytic degradation of CIP were investigated in the presence of Nano-GO/M nanoparticles. As the CIP concentrations were increased from 1 mg/L to 3 and 5 mg/L, the CIP adsorption yields increased slightly from 15% to 16.7% and 17% as the Nano-GO/M composite concentrations were increased from 0.5 g/L to 2.0 and 10 g/L, respectively, after 30 min at pH = 6.5 at 21°C. However, since the cost of 2 and 10 g/L Nano-GO/M composites is higher than that of 1 g/L Nano-GO/M composite, and only slightly higher CIP yields were obtained; for maximum CIP adsorption yield (15%), the optimum Nano-GO/M composite concentration was accepted as 0.5 g/L for CIP concentrations varying between 1 and 1,000 mg/L. The maximum adsorption capacities of Nano-GO/M varied between 2 and 2.20 mg_{CIP}/g_{Nano-GO/M} as the CIP concentrations were increased from 1 to 1,000 mg/L CIP at an optimum contact time of 30 min at pH = 6.5. Under acidic and basic conditions, the CIP adsorption yields decreased. Significantly higher CIP removal efficiencies were found under photocatalytic conditions compared with the adsorption process. The CIP photodegradation yields increased slightly from 93% to 94% as the CIP concentrations were increased from 1 to 3 mg/L at 0.5 g/L Nano-GO/M concentration for pH = 6.5 after 30 min photodegradation time. As the Nano-GO/M concentration were increased from 0.5 g/L to 2 and 10 g/L, the CIP photodegradation yields increased from 93%–94% to 95%–96% and 97%–98%, respectively, for CIP concentrations 1 and 3 mg/L, respectively, at a pH of 6.5, at a UV power of 300 W and at a temperature of 21°C after 30 min irradiation time throughout photocatalytic degradation. Further increase of CIP levels to 100, 500 and 1,000 mg/L did not significantly affect the CIP yields. Maximum 94% CIP photodegradation yield was obtained at 1,000 mg/L CIP concentration for the same operational conditions given above. CIP photodegraded according to the second-order kinetic model. Photodegradation of the CIP was pH dependent. Alkaline and acidic conditions were not favorable for CIP removal under UV. It can be concluded that the Nano-GO/M composite can be produced easily under laboratory conditions and can be used to treat some other fluoroquinolone group antibiotics and pharmaceuticals.

Acknowledgment

The authors would like to express appreciation for the support of the sponsors Dokuz Eylul University Scientific Research Project (KB.FEN.020) and TUBITAK 2210-C National Grant for a master thesis relevant to priority subjects.

Symbols

q_e	— Capacity of adsorbent, mg/g
C_0	— Initial liquid concentration, mg/L
C_e	— Equilibrium liquid concentration, mg/L
V	— Volume of solution, L
W	— Weight of adsorbent, g
k_{CIP/HO°	— Second-order reaction kinetic rate constant, min ⁻¹
$[HO^\circ]$	— Steady-state hydroxyl radical concentration in CIP solution under photocatalytic process, µg/ml

k	— Experimental pseudo-first-order reaction kinetic rate constant for CIP photodegradation, min
t	— Photodegradation time, min
$[CIP]$	— CIP concentration, µg/ml
q_m	— Maximum capacity of adsorbent
K_L	— Langmuir isotherm constant
K_F	— Freundlich constant, unitless
n	— Adsorption intensity, unitless
k	— First-order rate constant, 1/s
A_0	— Influent concentration of CIP, mg/L
A	— Effluent concentration of CIP, mg/L
t	— Time, min
k_1	— Constant of pseudo-first-order reaction, min ⁻¹
k_2	— Constant of pseudo-second-order reaction, min ⁻¹

References

- [1] J. Kagle, A.W. Porter, R.W. Murdoch, G. Rivera-Cancel, A.G. Hay, Biodegradation of pharmaceutical and personal care products, *Adv. Appl. Microbiol.*, 67 (2009) 65–108.
- [2] A. Bhandari, L.I. Close, W. Kim, R.P. Hunter, D.E. Koch, R.Y. Surampalli, Occurrence of ciprofloxacin, sulfamethoxazole, and azithromycin in municipal wastewater treatment plants, *Pract. period. hazard., toxic, radioact. Waste Manage.*, 12 (2008) 275–281.
- [3] D.G. Larsson, C. de Pedro, N. Paxeus, Effluent from drug manufactures contains extremely high levels of pharmaceuticals, *J. Hazard. Mater.*, 148 (2007) 751–755.
- [4] J.B. Belden, J.D. Maul, M.J. Lydy, Partitioning and photodegradation of ciprofloxacin in aqueous systems in the presence of organic matter, *Chemosphere*, 66 (2007) 1390–1395.
- [5] S. P. Sun, H. Q. Guo, Q. Ke, J. H. Sun, S. H. Shi, M. L. Zhang, and Q. Zhou. Degradation of antibiotic ciprofloxacin hydrochloride by photo-fenton oxidation process, *Environ. Eng. Sci.*, 26 (2009) 753–759.
- [6] N. Carmosini, S.L. Lee, Ciprofloxacin sorption by dissolved organic carbon from reference and bio-waste materials, *Chemosphere*, 77 (2009) 813–820.
- [7] B. De Witte, H. Van Langenhove, K. Demeestere, K. Saerens, P. De Wispelaere, J. Dewulf, Ciprofloxacin ozonation in hospital wastewater treatment plant effluent: effect of pH and H₂O₂, *Chemosphere*, 78 (2010) 1142–1147.
- [8] C.J. Wang, Z.H. Li, W.T. Jiang, Adsorption of ciprofloxacin on 2:1 dioctahedral clay minerals, *Appl. Clay Sci.*, 53 (2011) 723–728.
- [9] S.A.C. Carabineiro, T. Thavorn-Amornsri, M.F.R. Pereira, J.L. Figueiredo, Adsorption of ciprofloxacin on surface-modified carbon materials, *Water Res.*, 45 (2011) 4583–4591.
- [10] W. Shaoling, Z. Xindong, L. Yanhui, Z. Chunting, D. Qiuju, S. Jiankun, W. Yonghao, P. Xianjia, X. Yanzhi, W. Zonghua and X. Linhua, Adsorption of ciprofloxacin onto biocomposite fibers of graphene oxide/calcium alginate, *Chem. Eng. J.*, 230 (2013) 389–395.
- [11] S. Yuan Yuan, Y. Qinyan, G. Baoyu, G. Yuan, X. Xing, L. Qian, W. Yan, Adsorption and cosorption of ciprofloxacin and Ni(II) on activated carbon-mechanism study, *J. Taiwan Inst. Chem. Eng.*, 45 (2014) 681–688.
- [12] B. Madhuleena, S. Roy, S. Mitra, Desalination across a graphene oxide membrane via direct contact membrane distillation, *Desalination*, 378 (2016) 37–43.
- [13] Y. Zhen, Y. Han, Y. Hu, L. Haibo, L. Aimin, C. Rongshi, Flocculation performance and mechanism of graphene oxide for removal of various contaminants from water, *Water Res.*, 47 (2013) 3037–3046.
- [14] H. Chen, B. Gao, H. Li, Removal of sulfamethoxazole and ciprofloxacin from aqueous solutions by graphene oxide, *J. Hazard. Mater.*, 282 (2015) 201–207.
- [15] L. Dong, Z. Zhu, Y. Qiu, J. Zhao, Removal of lead from aqueous solution by hydroxyapatite/magnetite composite adsorbent, *Chem. Eng. J.*, 165 (2010) 827–834.

- [16] S. Rakshit, D. Sarkar, E. Elzinga, P. Punamiya, R. Datta, Mechanisms of ciprofloxacin removal by nano-sized magnetite, *J. Hazard. Mater.*, 246–247 (2013) 221–226.
- [17] Y. Tang, H. Guo, L. Xiao, S. Yu, N. Gao, Y. Wang, Synthesis of reduced graphene oxide/magnetite composites and investigation of their adsorption performance of fluoroquinolone antibiotics, *Colloids Surf., A*, 424 (2013) 74–80.
- [18] Y. Gao, L. Zhang, H. Huang, J. Hu, S. Shah, X. Su, Adsorption and removal of tetracycline antibiotics from aqueous solution by graphene oxide, *J. Colloid Interface Sci.*, 1 (2012) 540–546.
- [19] A. Mostofizadeh, Y. Li, B. Song and Y. Huang, Synthesis, properties, and applications of low dimensional carbon-related nanomaterials, *J. Nanomater.* 2011(3), (2011) Article ID 685081, 21 pages <http://dx.doi.org/10.1155/2011/685081>
- [20] A. Lunhong, Z. Chunying, C. Zhonglan, Removal of methylene blue from aqueous solution by a solvothermal-synthesized graphene/magnetite composite, *J. Hazard. Mater.*, 192 (2011) 1515–1524.
- [21] Y. Nengsheng, X. Yali, S. Pengzhi, G. Ting, M. Jichao, Synthesis of magnetite/graphene oxide/chitosan composite and its application for protein adsorption, *Mater. Sci. Eng., C*, 45 (2014) 8–14.
- [22] B. David, Sonochemical degradation of PAH in aqueous solution. Part I: Monocomponent PAH solution, *Ultrason. Sonochem.*, 16 (2009) 260–265.
- [23] M. Yahya, N. Oturan, K. Kacemi, M. Karbane, C.T. Aravindakumar, M. Oturan, Oxidative degradation study on antimicrobial agent ciprofloxacin by electro-Fenton process: kinetics and oxidation products, *Chemosphere*, 117 (2014) 447–454.
- [24] Wikipedia, (2016a). Rate equation. Retrieved June, 22, 2016 from https://en.wikipedia.org/wiki/Rate_equation
- [25] Q. Huamin, L. Chuannan, S. Min, L. Fuguang, F. Lulu, L. Xiangjun, A chemiluminescence sensor for determination of epinephrine using graphene oxide–magnetite-molecularly imprinted polymers, *Carbon*, 50 (2012) 4052–4060.
- [26] M. Zhang, D. Lei, X. Yin, L. Chen, Q. Li, Y. Wang, T. Wang, Magnetite/graphene composites: microwave irradiation synthesis and enhanced cycling and rate performances for lithium ion batteries, *J. Mater. Chem.*, 20 (2010) 5538–5543.
- [27] Y. Li, Q. Du, J. Wang, T. Liu, J. Sun, Y. Wang, Z. Wang, Y. Xia, L. Xia, Defluoridation from aqueous solution by manganese oxide coated graphene oxide, *J. Fluorine Chem.*, 148 (2013) 67–73.
- [28] F. Wang, B. Yang, H. Wang, Q. Song, F. Tan, Y. Cao, Removal of ciprofloxacin from aqueous solution by a magnetic chitosan grafted graphene oxide composite, *J. Mol. Liq.*, 222 (2016) 188–194. doi: 10.1016/j.molliq.2016.07.037
- [29] S. Wu, X. Zhao, Y. Li, C. Zhao, Q. Du, J. Sun, Adsorption of ciprofloxacin onto biocomposite fibers of graphene oxide/calcium alginate, *Chem. Eng. J.*, 230 (2013) 389–395.
- [30] S.A.C. Carabineiro, T. Thavorn-amornsri, M.F.R. Pereira, P. Serp, J.L. Figueiredo, Comparison between activated carbon, carbon xerogel and carbon nanotubes for the adsorption of the antibiotic ciprofloxacin, *Catal. Today*, 186 (2012) 29–34.
- [31] Z. Hong, L. Donghong, Z. Yan, L. Shuping, L. Zhe, Sorption isotherm and kinetic modeling of aniline on Cr-bentonite, *J. Hazard. Mater.*, 167 (2009) 141–147.
- [32] X. Wang, H. Ngo, W. Guo, Preparation of a specific bamboo based activated carbon and its application for ciprofloxacin removal, *Sci. Total Environ.*, 533 (2015) 32–333.
- [33] N. Genc, E. Dogan, Adsorption kinetics of the antibiotic ciprofloxacin on bentonite, activated carbon, zeolite, and pumice, *Desal. Wat. Treat.*, 53 (2015) 785–793.
- [34] C. Gu, K. Karthikeyan, Sorption of the antimicrobial ciprofloxacin to aluminum and iron hydrous oxides, *Environ. Sci. Technol.*, 39 (2005) 9166–9173.
- [35] C.J. Wang, Z.H. Li, W.T. Jiang, J.S. Jean, C.C. Chuan, Cation exchange interaction between antibiotic ciprofloxacin and montmorillonite, *J. Hazard. Mater.*, 183 (2010) 309–314.
- [36] M. Jalil, M. Baschini, K. Sapag, Influence of pH and antibiotic solubility on the removal of ciprofloxacin from aqueous media using montmorillonite, *Appl. Clay Sci.*, 114 (2015) 69–76.
- [37] G. Liu, N. Wang, J. Zhou, A. Wang, J. Wang, R. Jin, L. Hong, Microbial preparation of magnetite/reduced graphene oxide nanocomposites for the removal of organic dyes from aqueous solutions, *RSC Adv.*, 5 (2015) 95857–95865.
- [38] D. Sponza, R. Oztekin, Ciproxin Removal from a Raw Wastewater by Nano Bentonite-ZnO: Comparison of Adsorption and Photooxidation Processes, *Recent Advances in Environmental and Biological Engineering*, 2014, ISBN: 978-1-61804-259-0.
- [39] M. Pelaez, N. Nolan, S. Pillai, M. Seery, P. Falaras, A. Kontos, P. Dunlop, J. Hamilton, J. Byrne, K. O’Shea, M. Entezari, D. Dionysiou, A review on the visible light active titanium dioxide photocatalysts for environmental applications, *Appl. Catal., B*, 125 (2012) 331–349.
- [40] L. Zhe-Qi, W. Hui-Long, Z. Long-Yun, Z. Jian-Jun, Z. Yao-Shan, Preparation and photocatalytic performance of magnetic TiO₂-Fe₃O₄/graphene (RGO) composites under VIS-light irradiation, *Ceram. Int.*, 41 (2015) 10634–10643.
- [41] L. Xinlin, L. Peng, Y. Guanxin, M. Changchang, T. Yangfeng, W. Yuting, H. Pengwei, P. Jianming, S. Weidong, Y. Yongsheng, Selective degradation of ciprofloxacin with modified NaCl/TiO₂ photocatalyst by surface molecular imprinted technology, *Colloids Surf., A*, 441 (2014) 420–426.
- [42] Y. Yan, S. Shaofang, S. Yang, Y. Xu, G. Weisheng, L. Xinlin, S. Weidong, Microwave-assisted in situ synthesis of reduced graphene oxide-BiVO₄ composite photocatalysts and their enhanced photocatalytic performance for the degradation of ciprofloxacin, *J. Hazard. Mater.*, 250–251 (2013) 106–114.
- [43] R. Upadhyay, N. Soin, S. Roy, Role of graphene/metal oxide composites as photocatalysts, adsorbents and disinfectants in water treatment: a review, *RSC Adv.*, 114 (2013) 69–76.
- [44] C. Lin, M. Wu, Degradation of ciprofloxacin by UV/S₂O₈²⁻ process in a large photoreactor, *J. Photochem. Photobiol., A*, 285 (2014) 1–6.
- [45] A. Hassani, A. Khataee, S. Karaca, Photocatalytic degradation of ciprofloxacin by synthesized TiO₂ nanoparticles on montmorillonite: effect of operation parameters and artificial neural network modeling, *J. Mol. Catal.*, 409 (2015) 149–161.
- [46] N. Daneshvar, S. Aber, M.S. Dorraji, R. Khataee, H. Rasoulifard, Photocatalytic degradation of the insecticide diazinon in the presence of prepared nanocrystalline ZnO powders under irradiation of UV-C light, *Sep. Purif. Technol.*, 58 (2007) 91–98.
- [47] L. Yang, L. Yu, M. Ray, Degradation of paracetamol in aqueous solutions by TiO₂ photocatalysis, *Water Res.*, 42 (2008) 3480–3488.
- [48] Y. Wang, G. Von, D.H. Volman, D.C. Neckers, *Advances in Photochemistry*, Bünau, Ed., Wiley, New York, 1995, pp. 179–234.
- [49] T. An, H. Yang, G. Li, W. Song, W. Cooper, X. Nie, Kinetics and mechanism of advanced oxidation processes (AOPs) in degradation of ciprofloxacin in water, *Appl. Catal., B*, 94 (2010) 288–294.